Structural Basis for Nucleotide-dependent Regulation of Membrane-associated Guanylate Kinase-like Domains*

Yuanhe Li‡, Oliver Spangenberg§, Ingo Paarmann§, Manfred Konrad§, and Arnon Lavie‡¶

*From the ‡Department of Biochemistry and Molecular Biology, University of Illinois at Chicago, Chicago, Illinois 60607
and the §Department of Molecular Genetics, Max Planck Institute for Biophysical Chemistry, Göttingen 37018, Germany*

CASK is a member of the membrane-associated guanylate kinases (MAGUK) homologs, a family of proteins that scaffold protein complexes at particular regions of the plasma membrane by utilizing multiple protein-binding domains. The GK domain of MAGUKs, which shares high similarity in amino acid sequence with yeast guanylate kinase (yGMPK), is the least characterized MAGUK domain both in structure and function. In addition to its scaffolding function, the GK domain of hCASK has been shown to be involved in transcription regulation. Here we report the crystal structure of the GK domain of human CASK (hCASK-GK) at 1.3-Å resolution. The structure rationalizes the inability of the GK domain to catalyze phosphoryl transfer and strongly supports its new function as a protein-binding module. Comparison of the hCASK-GK structure with the available crystal structures of yGMPK provides insight into possible conformational changes that occur in hCASK upon GMP binding. These conformational changes may act to regulate hCASK-GK function in a nucleotide-dependent manner.

Membrane-associated guanylate kinases (MAGUKs)[1] constitute a newly recognized class of proteins found in all animals examined to date. They act as molecular scaffolds for signaling pathway components, regulate synaptic structure and function by mediating specific interactions, and (in *Drosophila*) act as tumor suppressors. In addition, MAGUKs recruit molecules into localized multimolecular complexes and cluster these complexes at the plasma membrane, such as cell junctions or the apicolateral or basolateral surface, and pre- or post-synaptic sites (1–6). All MAGUK proteins share a similar multidomain structural organization that includes (from the N to C termini) one or three copies of PDZ (PSD-95/SAP-90-Dlg-Zo1) domains, followed by one Src homology 3 (SH3) domain, then followed by a guanylate kinase-like (GK) domain (3). The PDZ domain functions as a protein-protein interaction module and is typically involved in the assembly of supramolecular complexes that perform localized signaling functions at particular subcellular locations (7). Although their specific functions in MAGUKs are not very clear, SH3 domains are found in many other proteins and are recognized as modular protein-protein interaction domains with an affinity for certain proline-rich motifs (8).

The GK domain in MAGUKs shares high sequence similarity with yeast guanylate kinase (yGMPK), a nucleoside monophosphate kinase that converts GMP to GDP using ATP as a phosphate donor. However, no enzymatic activity is present in MAGUK GK domains. Moreover, several protein binding partners of GK domains were found by yeast two-hybrid screens or pull-down assays (see Table III below), and this suggested that the GK domain functions as a protein-binding module. Although the GK domain cannot catalyze phosphoryl transfer, it can bind nucleotides. Binding studies have shown that the GK domain of SAP-90 binds GMP in the micromolar range and ATP in the millimolar range (9). Although a GK domain is present in all MAGUKs, there is remarkable divergence in nucleotide-binding sites among the four MAGUK subfamilies (see Fig. 1 below): Lin2/CASK- and p55-like MAGUKs have nearly intact GMP- and ATP-binding sites; Dlg/SAP-90- and SAP-97-like MAGUKs have conserved GMP-binding sites but lack some residues in their ATP-binding site; the ZO1-like MAGUKs lack some residues in both sites (3). The role of nucleotide binding to the GK domain is unclear in the absence of any enzymatic activity. Based on known nucleotide-dependent conformational changes that were observed in several nucleoside monophosphate kinases, we hypothesized that nucleotides could play a regulatory role in GK function by inducing different conformations between the nucleotide-free and nucleotide-bound forms

To test this hypothesis we commenced crystallographic studies of GK domains from different MAGUKs. Here we report the 1.3-Å crystal structure of the GK domain of human CASK (hCASK-GK). Comparison of this structure, which is the first MAGUK GK domain elucidated to our knowledge, with the structures of yGMPK with and without GMP reveals important differences in the conformation of the GMP-binding region and the LID region. The structure reveals the reasons hCASK-GK is not able to catalyze phosphoryl transfer. Modeling of GMP into hCASK-GK strongly supports the binding of GMP to hCASK-GK. The hCASK-GK crystal structure and the hCASK-GK-GMP model here reveal how an enzyme has been converted

The atomic coordinates and structure factors (code 1KGD) have been deposited in the Protein Data Bank, Research Collaboratory for Structural Bioinformatics, Rutgers University, New Brunswick, NJ (http://www.rcsb.org/).

¶ To whom correspondence should be addressed: Dept. of Biochemistry and Molecular Biology, University of Illinois at Chicago, 1819 West Polk St., Chicago, IL 60612. Tel.: 312-355-5029; Fax: 312-355-4535; E-mail: lavie@uic.edu.

[1] The abbreviations used are: MAGUK, membrane-associated guanylate kinase; PDZ, PSD-95/SAP-90-Dlg-Zo1 domain; SH3, Src homology 3; GK, guanylate kinase-like domain; yGMPK, yeast guanylate kinase; hCASK-GK, GK domain of human CASK; r.m.s.d., root mean square deviation; MAD, multiwavelength anomalous diffraction method.

into a protein-binding module and suggest how binding to GMP could regulate the conformational state of this module within multidomain proteins.

<div style="text-align: center;">EXPERIMENTAL PROCEDURES</div>

Cloning and Recombinant Expression of hCASK-GK—A cDNA encoding the GK domain from human CASK protein (hCASK-GK; Arg-734 to Cys-909) was amplified by the polymerase chain reaction from a pCRII plasmid (Invitrogen Corp.), containing a full-length cDNA of hCASK (10), and cloned into a modified pGEX-2T (Amersham Biosciences, Inc.) *E. coli* expression vector, which allowed insertion of *Nde*I/*Bam*HI-restricted fragments into its multiple cloning site (11).

Protein Expression and Purification—*Escherichia coli* BL21(DE3) cells carrying the plasmid that contains the gene encoding the hCASK-GK-GST fusion protein were induced by 0.1 mM isopropyl-β-D-thioga-lactopyranoside for 6 h at 25 °C in 2YT media. Cells were harvested by centrifugation and lysed with lysozyme, and the supernatant after ultracentrifugation was applied to a glutathione *S*-transferase-Sepharose column pre-equilibrated with 50 mM Tris-HCl, pH 7.5, 200 mM KCl, 5 mM MgCl$_2$, 1 mM EDTA, and 10 mM dithiothreitol. After washing, the fusion protein was cleaved on the column with thrombin for about 24 h. The flow-through was collected and further purified to homogeneity by using an ion exchange column (WP-QUAT) and gel filtration (Superdex-75). The protein was concentrated by ultrafiltration to 25 mg/ml. Because of the construction of a thrombin cleavage site at the N-terminal of hCASK-GK, the resultant protein after cleavage has four additional amino acids (Gly-Ser-His-Met-) at the N terminus. For seleno-methionine-containing protein, the plasmid was transformed into the methionine auxotroph *E. coli* strain B834(DE3), and the cells were grown and induced as described previously (12). Purification was conducted as with the non-labeled protein. Incorporation of seleno-methionine at all four positions was confirmed by mass spectroscopy.

Crystallization—Crystals were obtained by the hanging-drop method at 20 °C. One microliter of 4 M sodium formate (the reservoir solution) was mixed with an equal volume of 15 mg/ml of the protein in 50 mM Tris-HCl, pH 7.5, 200 mM KCl, 5 mM MgCl$_2$, 1 mM EDTA, and 10 mM dithiothreitol. Initial crystals were found after 2 weeks. Further crystals were obtained with microseeding. Trigonal crystals appeared overnight and grew to a maximum size of 350 × 350 × 400 μm^3 in 1 week. The Matthews coefficient of 2.73 (55% solvent content) suggested a monomer as the asymmetric unit (13). Seleno-methionine crystals were grown from seleno-methionine containing hCASK-GK protein using the microseeding technique.

Data Collection—Initial native diffraction data to 1.6-Å resolution were collected on a RAXIS IIc image plate detector using copper radiation from a RAXIS RU-200 rotation anode x-ray generator at 100 K. The cryoprotectant was mineral oil. Molecular replacement with the yGMPK model failed, a fact explained by our structure of the CASK-GK domain that reveals large differences and movement of the GMP-binding region and LID region. MIR was tried but also failed due to lack of isomorphism. Therefore, a MAD dataset was collected from a crystal grown from seleno-methionine-labeled protein at three different wavelengths (inflection, maximum, and high energy) at the BIOCars beamline BM-D in the Advanced Photon Source, Argonne National Laboratory using a Quantum-4 charge-coupled device detector at 100 K. This seleno-methionine crystal was grown with continuous microseeding, and it diffracted to 1.7 Å. In addition, a native dataset at 1.31 Å was also collected. The data were processed with DENZO/SCALEPACK (14).

Structure Determination and Refinement—The crystal structure of hCASK-GK was solved using the MAD dataset collected from a seleno-methionine crystal. At this stage the space group ambiguity between p3$_1$21 and p3$_2$21 was solved, the latter being the correct space group. All of the four selenium sites in one hCASK-GK monomer were located by the program SOLVE (15). The resulting phases were improved with DM (16). Automatic model building was done with ARP (17). Manuel model adjustment was carried out with the graphics package O (18). The structure was initially refined with CNS (19) against the MAD data in the resolution range 12.0–1.7 Å. 10% data were used for R_{free} calculations. The model was then refined against the higher resolution native data set. Following rigid-body, minimization, annealing, and *B*-factor refinement, the model was checked with $2F_o - F_c$ and $F_o - F_c$ maps. After several iterations of refinement with CNS, anisotropic *B*-factor refinement was done with REFMAC5.0 (20). Coordinates and structure factors were being deposited in the Protein Data Bank (PDBID 1KGD).

Modeling of GMP into the Structure of hCASK-GK—We modeled GMP into the structure of hCASK-GK guided by the structure of
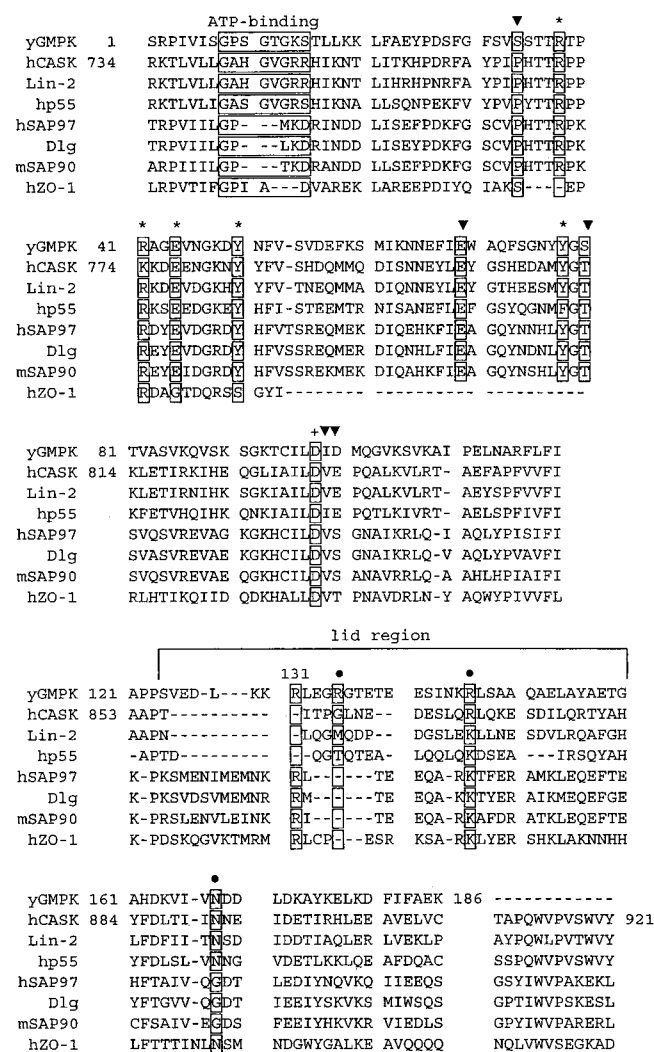
FIG. 1. **Sequence alignment of the GK domain of MAGUKs and yGMPK.** The alignment was done using the Multalin Interface Page and further edited manually (39). The glycine-rich ATP binding motif and residues responsible for binding of guanine ring (▼), phosphates (*) of GMP, and for binding of Mg^{2+}(+) are boxed as well as the residues involved in catalysis (Arg-135, Arg-146, and Asn-168 in yGMPK, ●) and the residue responsible for ATP binding (Arg-131).

yGMPK with GMP (GMPK$_{\text{GMP}}$). Based on the high similarity of the CORE and GMP-binding regions between our hCASK-GK structure and the GMPK$_{\text{GMP}}$ structure, we could align the two structures once based on atoms only from the CORE region and once from atoms only from the GMP-binding region. We then made a chimera coordinate file from two hCASK-GK pdb files generated by these two operations, *i.e.* the CORE (and LID) regions from the pdb file after using the CORE regions for the superposition operation, and the GMP-binding region from the pdb file generated by using only atoms from the GMP-binding region for the superposition calculation. The location of the GMP molecule is exactly where it was in the GMPK$_{\text{GMP}}$ structure. Interactions between GMP and hCASK-GK side chains were optimized by rotating the side chains around their torsion angles.

<div style="text-align: center;">RESULTS</div>

Structure Determination of hCASK-GK—Human CASK-GK (Fig. 1) crystallizes in the hexagonal space group P3$_2$21 with one molecule in the asymmetric unit. The structure (Fig. 2) was solved using the multiwavelength anomalous diffraction method (MAD) (21). Data collection and phasing statistics can be found in Table I. The experimental electron density map was of very high quality, and the program ARP was successful in automatically building most of the hCASK-GK model (Fig. 3A). After manual rebuilding with the 1.7-Å MAD dataset, the res-
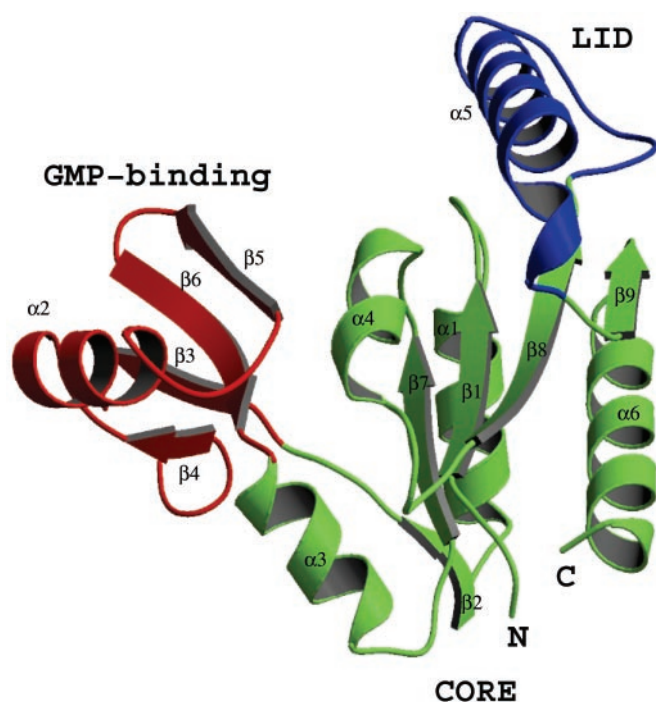
FIG. 2. **Overall structure of hCASK-GK.** *Green* represents the CORE region, strands β1, β2, β7, β8, and β9, and helices α1, α3, α4, and α6. *Red*, the GMP-binding region, composed of β3, β4, β5, β6, and helix α2. *Blue*, the LID region, helix α5. Structural figures were generated with BOBSCRIPT (40) and RASTER3D (41).

olution was extended by using the native 1.31-Å dataset. The final structure of hCASK-GK consists of 175 residues, 5 formate ions, and 218 water molecules. The N-terminal residues 730 and 731 (Gly-Ser) and residues 774–776 (Lys-Lys-Asp) did not have good electron density so were not modeled. The final crystallographic *R*-factor is 18.6% ($R_{\text{free}} = 21.2\%$) for all the reflections within the resolution range 12.0–1.31 Å. Refinement statistics are shown in Table I.

Overall Structure—The fold of hCASK-GK is similar to that of the yeast guanylate kinase (yGMPK) and, in a similar manner to the latter, can be divided into three dynamic regions (Fig. 2). The CORE region is built by five parallel β-strands and four α-helices. This region is flanked by the GMP-binding region (*red*) and the LID region (*blue*). The former is composed of a four-stranded β-sheet and a single α-helix, whereas the LID is seven residues shorter than in yGMPK and is composed of a long loop and one α-helix. The division of hCASK-GK into these three regions was guided by comparing our structure to known structures of yGMPK such that each region can move as a rigid body relative to the other regions. Therefore, our choice of regions is slightly different than those previously chosen for yGMPK, especially for the LID region (22). We have chosen helix α-5 to be a part of the LID region and not the CORE region, because it adopts a quite different conformation and position in hCASK from that in yGMPK.

Comparison between the Structures of hCASK-GK and yGMPK—Comparison of the hCASK-GK structure with the yeast guanylate kinase was performed against the ligand-free yGMPK (GMPK$_{apo}$) and the GMP-bound yGMPK structures (GMPK$_{GMP}$). For the structural alignment of the three structures, we only used atoms in the CORE region for the calculation of the transformation matrices. The result of these operations is shown in Fig. 3*B*. The CORE region of hCASK-GK shows high similarity to that of GMPK$_{apo}$ and GMPK$_{GMP}$ (Fig. 4*A*). For the 91 Cα atoms used for alignment, the root mean

square deviation (r.m.s.d.) is 2.368 and 2.462 Å between hCASK-GK and GMPK$_{apo}$ and GMPK$_{GMP}$, respectively.

However, the deviations between the other regions are pronounced. These deviations are due to conformational changes by which the GMP-binding region and the LID region move as rigid bodies relative to the CORE region. Using atoms only from the CORE domain for the superposition calculation shows that the GMP-binding region of hCASK-GK is positioned between the conformation it adopts in the open GMPK$_{apo}$ structure and the closed conformation in the GMPK$_{GMP}$ structure (Fig. 3*B*). However, if one performs the alignment using only the atoms from the GMP-binding region (Fig. 4*B*), the resulting structural overlay reveals that the basic structure of the GMP-binding region is nearly identical between all three structures (r.m.s.d. is 0.719 Å between hCASK-GK and GMPK$_{apo}$ and 0.802 Å between hCASK-GK and GMPK$_{GMP}$ for the 45 Cα atoms). This was previously demonstrated for the two yGMPK structures (22), and our result shows that the GK domain of hCASK maintains a nearly identical GMP-binding region to that of yGMPK, albeit it is in a different conformation relative to the CORE region from those previously observed for GMPK$_{apo}$ or GMPK$_{GMP}$. Because in our structure of hCASK-GK the nucleotide GMP is absent, our result suggests an attractive mechanism in which the function of MAGUKs may be regulated.
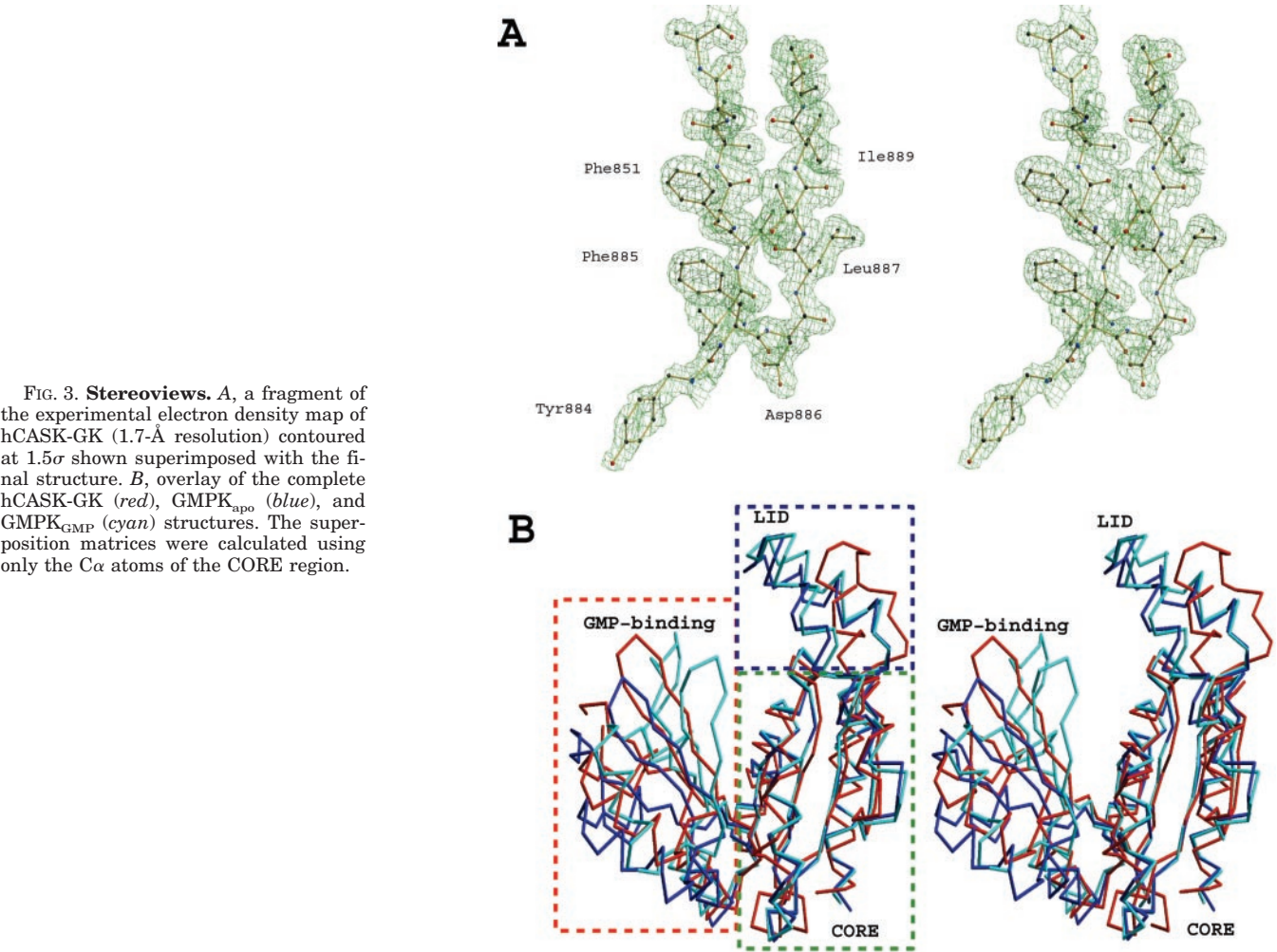
The above operation for the superposition of the GMP-binding regions can be repeated for the LID regions, but the result is very different. Not surprisingly, the LID of yeast guanylate kinase in the apo- and GMP-bound structures overlay with a very low r.m.s.d. However, the shorter LID region of hCASK adopts a very different conformation from that of the enzyme guanylate kinase (Fig. 4*C*). The LID region of GMPK$_{apo}$ and GMPK$_{GMP}$ is composed of two helices connected by a loop, whereas the LID region of hCASK-GK is composed of only a single helix and a long loop. The overlay done by using the CORE region to align the structures shows that the LID region of hCASK-GK cannot be superimposed on the LID regions of GMPK$_{apo}$ or GMPK$_{GMP}$ (Fig. 3*B*). Moreover, even if the calculation of the superposition matrix is performed using the most similar feature between the LID regions, the α-helix, no good superposition is obtained (Fig. 4*C*). Thus, unlike the difference in structure between the GMP-binding region of hCASK-GK and yGMPK, which can be explained by a rigid-body conformational change, the LID region of hCASK is structurally distinct from that of yGMPK. This fact serves to explain the apparent inability of hCASK-GK to catalyze phosphoryl transfer (see "Discussion") and of the MAGUK SAP-97 even after reconstituting the P-loop region (23).

Modeling of GMP Binding into the Structure of hCASK-GK—Our structure of hCASK-GK does not contain the nucleotide GMP. *In vitro* binding studies of SAP-90 and SAP-97 have shown that GMP can bind to the GK domain (9, 23). Modeling of GMP binding to hCASK-GK was guided by the hypothesis that upon GMP binding the conformation of hCASK-GK would change to a more closed one, as was seen upon binding of GMP to yGMPK. Using the GMPK$_{GMP}$ structure as a guide, we were able to model the expected closed conformation of hCASK-GK (Fig. 5*A*). In our model of GMP-bound hCASK-GK, the main difference with the yGMPK GMP-bound structure is the position and fold of the LID region. Both the CORE region and the GMP-binding region overlay well. Except for residues Ser-34 and Arg-41, all other residues observed to interact with GMP in the GMPK$_{GMP}$ structure are found almost at the same position in the hCASK-GK-GMP model. The apparent lack of a residue that would correspond to Arg-41 of yGMPK can be explained by the fact that we could not observe traceable electron density for

TABLE I
Summary of data collection, phasing, and refinement statistics

	Native $\lambda = 1.0$ Å	Edge $\lambda = 0.97788$ Å	Peak $\lambda = 0.97765$ Å	Remote $\lambda = 0.95520$ Å
Data set				
Resolution (Å)	1.31	1.7	1.7	1.7
Measured reflections	327,011	199,357	194,509	200,270
Unique reflections	48,853	53,889	53,364	54,314
Completeness (%)[a]	94.2 (81.0)	99.6 (100)	99.7 (100)	99.9 (100)
I/σ[a]	20.9 (8.31)	25.1 (6.2)	23.9 (4.7)	19.2 (6.2)
R_{sym} (%)[b]	3.4 (14.5)	3.7 (22.6)	4.2 (30.4)	3.7 (26.4)
Overall figure of merit[c]		0.47 (0.61)		
Space group	p3$_2$21			
Unit cell dimensions (Å)	a = b = 70.341			
	c = 74.8611			
Refinement				
R-factor/R_{free}	18.6/21.2			
Resolution range	12–1.31			
No. of protein atoms/water molecules/formate r.m.s.d.	1466/218/5			
Bond lengths (Å)	0.0055			
Bond angles (°)	2.371			
Overall B-factor (Å^2)	25.77			

[a] Overall and last shell is in parentheses.
[b] $R_{sym} = \Sigma|(I - I)|/\Sigma(I)$, where I is the observed intensity.
[c] Overall figure of merit after SOLVE and after phase extension is in parentheses.

FIG. 3. **Stereoviews.** *A*, a fragment of the experimental electron density map of hCASK-GK (1.7-Å resolution) contoured at 1.5σ shown superimposed with the final structure. *B*, overlay of the complete hCASK-GK (*red*), GMPK$_{apo}$ (*blue*), and GMPK$_{GMP}$ (*cyan*) structures. The superposition matrices were calculated using only the Cα atoms of the CORE region.

residues 774–776 of hCASK-GK. Lysine 774, which is not present in our model, would correspond to Arg-41 of yGMPK. Our inability to model the above loop is consistent with the expectation that this loop would become more ordered once GMP binds to hCASK-GK. Fig. 5*B* shows the superposition of the residues responsible for GMP binding in GMPK$_{GMP}$ and in

our hCASK-GK-GMP model. The expected interactions between GMP and hCASK-GK are listed in Table II.

DISCUSSION

An impressive amount of information on the structural and functional networks that underlie neuronal activity has recently
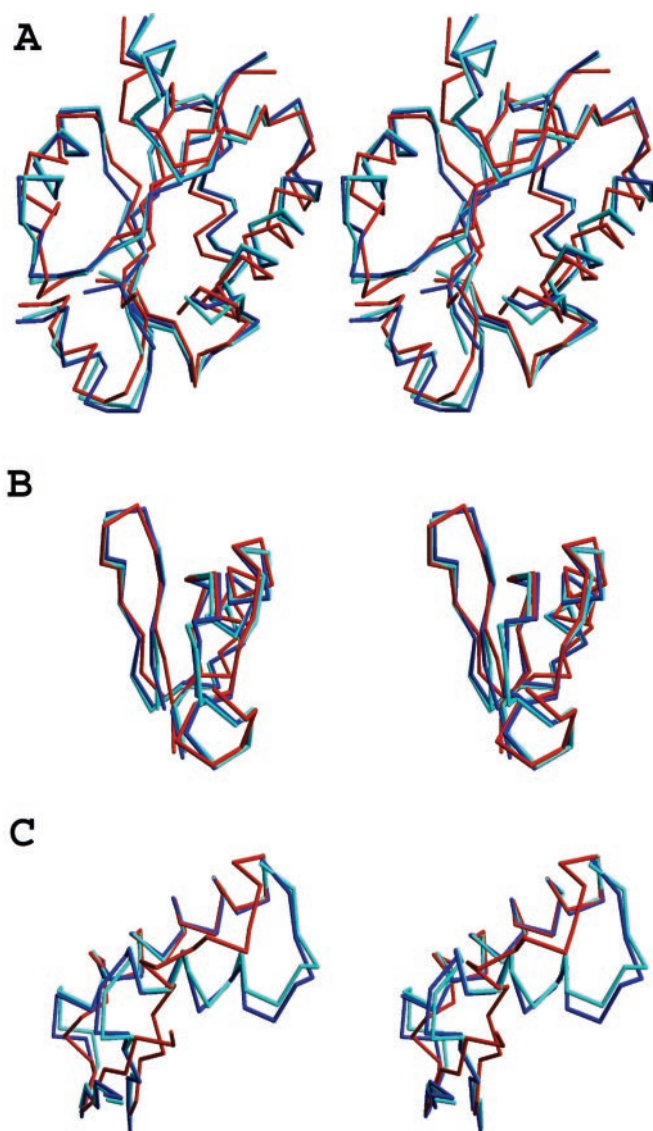
has no enzymatic activity.

Several protein binding partners of GK domains were found by yeast two-hybrid screens or pull-down assays (Table III), and this suggested that the GK domain functions as a protein binding module. Remarkably, several MAGUKs and interacting proteins have additional, recently discovered biological functions: GAKIN is a member of the kinesin superfamily of motor proteins, and its interaction with the GK domain seems to play a vital role in the intracellular trafficking of hDlg (28). CASK, a member of the Lin2-like MAGUKs, has a transcription regulation function through interaction of its GK domain with Tbr-1, a T-box transcription factor that is involved in forebrain development (29). The GK domain is also involved in inter- and intramolecular interaction with MAGUK's SH3 domain, and this intramolecular interaction regulates SAP-97 binding to GKAP and PSD-95/SAP-90 clustering of ion channels (30–33). In addition, it is known that the *Drosophila* Dlg protein, the prototype member of the MAGUK family, is required in the maintenance of septate junctions and epithelial structure; mutations in the SH3 and GK domains of the protein are oncogenic in larval development, and deletions in the GK domain cause loss of normal growth without affecting epithelial structure (34–36). Similarly, the GK domains of murine Dlg/SAP-97 and of CASK are essential to craniofacial and palatal morphogenesis in mice (37). Because these interactions and functions were shown to be restricted to the GK domains of the respective MAGUK subfamilies, it can be assumed that their specificity is determined by subtle differences in GK domain structures. The high resolution structure of the CASK GK domain we present in this study will allow to gain insights into the molecular basis of the distinct mechanisms for the interactions between the GK domains and their binding partners.

Despite having only 27% sequence identity with yGMPK, the structure of hCASK-GK shows that the CORE and GMP-binding regions are markedly similar. The most apparent difference between the two proteins is the LID region, a region that in the enzyme yGMPK contains essential residues for catalysis. Similarly, the essential role of particular arginine residues from the LID region was highlighted in our previous work on thymidylate kinase (11, 38). LID region yGMPK arginines play a role in ATP binding (Arg-131) and in stabilizing the phosphate groups of ATP in the catalytic transition state (Arg-135 and Arg-146). None of the MAGUKs retain all of these three arginines (Fig. 1). The LID region of hCASK-GK has only a single arginine (Arg-869), which the structure-based sequence alignment suggests could correspond to the catalytic Arg-146 of yGMPK. However, the structure of hCASK-GK reveals that this arginine extends toward a totally different direction from that of Arg-146 observed in the structures of yGMPK. This is unlikely due to the lack of nucleotide in our hCASK-GK structure because this residue adopts a similar orientation in both the apo- and GMP-bound yGMPK structures. This shows that the LID region of hCASK-GK is deficient in residues essential for catalyzing phosphoryl transfer. Importantly, our structures show no other residues from other parts of the molecule that could compensate for the lack of these arginine residues. Therefore, our structural analyses yield an explanation for the lack of guanylate kinase activity of the GK domain of MAGUKs.

Although it is now understood why the GK domain cannot catalyze phosphoryl transfer, the question remains: Can it bind ATP or GMP? Our equilibrium binding assays show that hCASK-GK binds GMP with a dissociation constant of 0.3 μM but binds ATP with a dissociation constant greater than 10 mM.[2] These results are consistent with our structure analyses that

FIG. 4. **Stereoview of a Cα trace of the overlaid different regions of hCASK-GK, GMPK$_{apo}$, and GMPK$_{GMP}$ generated by using the Cα atoms of the different regions.** *Red*, hCASK-GK; *blue*, GMPK$_{GMP}$; *cyan*, GMPK$_{apo}$. *A*, the overlaid CORE regions of hCASK-GK, GMPK$_{apo}$, and GMPK$_{GMP}$ generated by using the Cα atoms of the CORE region of the three structures. *B*, the overlaid GMP-binding regions of hCASK-GK, GMPK$_{apo}$, and GMPK$_{GMP}$ generated by using the Cα atoms of the GMP-binding region of the three structures. *C*, overlaid LID regions made by using only Cα atoms of the helix in the LID region of the three structures. The LID region of hCASK is fundamentally different from that of yGMPK, and that observed difference is not a result of a simple rigid-body movement.

accumulated through proteomic approaches to the analysis of the molecular basis of synaptic signaling pathways (24, 25). A large number of proteins identified in signaling complexes, neuromuscular junctions, and cell-cell contact sites contain characteristic regions such as SH3 and PDZ domains. These domains mediate specific protein-protein interactions and form scaffolds for protein networks at specialized regions of the cell membranes. The MAGUK family constitutes a major group of conserved cytoskeletal proteins that consist of arrayed modular domains: one to three PDZ domains, an SH3 domain, and, as a signature motif, a C-terminal guanylate kinase-like domain. Whereas SH3 domains have a well-known role as protein interaction modules in other systems (26), and PDZ domains were recognized as adapters for clustering of transmembrane or membrane-associated proteins at high local concentrations (7, 27), the role of the GK domain has until recently been mysterious, given the fact that it

---

[2] O. Spangenberg, I. Paarmann, and M. Konrad, unpublished results.

FIG. 5. **Modeling of GMP into the hCASK-GK structure.** *A*, stereoview of the GMPK$_{GMP}$ (*cyan*) structure overlaid with the model GMP-bound hCASK-GK (*red* and *purple*). For details on model generation see the "Experimental Procedures." The *black arrow* shows the expected conformational change that would occur in hCASK-GK upon GMP binding. *B*, superposition of the GMP-binding sites in the GMP-bound model of hCASK-GK (*pink*) and GMPK$_{GMP}$ (*cyan*). The residues of hCASK-GK are labeled. See also Table II.
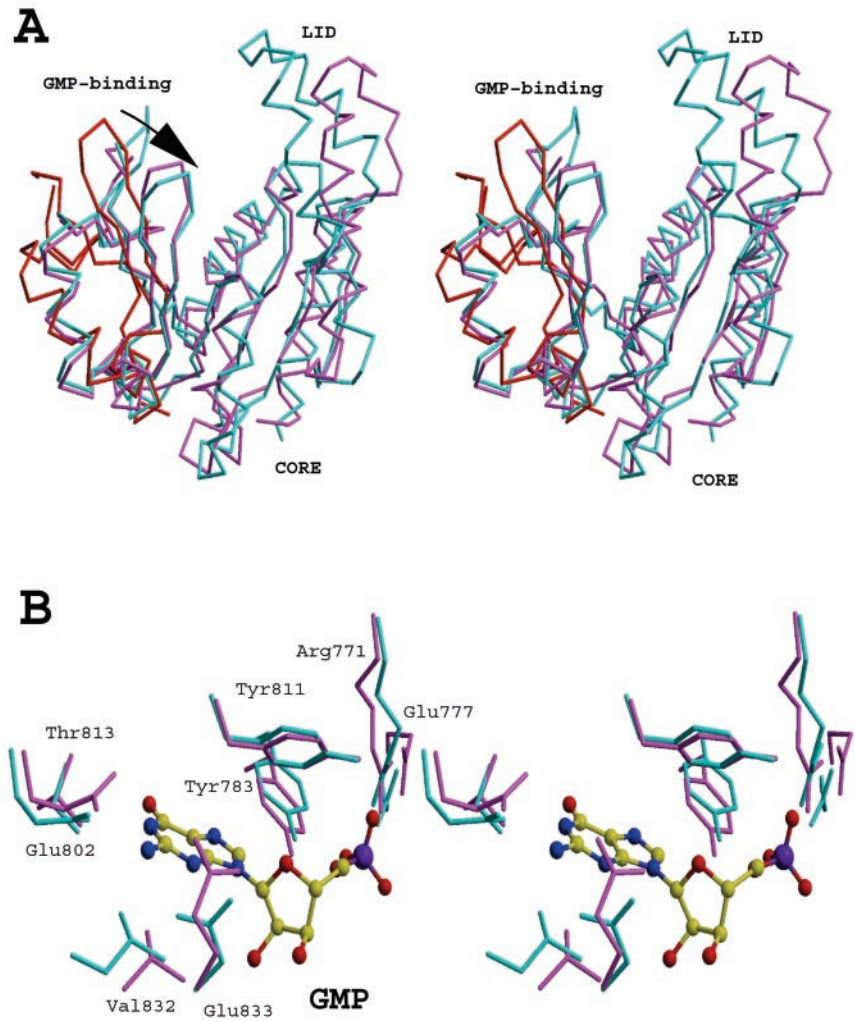
TABLE II
Interactions between GMP and hCASK (modeled) and yGMPK

Interactions are between GMP and side-chain atoms and were considered to take place if atoms were between 3.5 and 2.4 Å apart.

Nucleotide part of GMP making the interaction	Residue in GMPK$_{GMP}$	Corresponding residue in the hCASK-GK-GMP model
Guanine ring	Glu[69]	Glu[802]
	Tyr[78a]	Tyr[811a]
	Ser[80]	Thr[813]
	Ile[99a]	Val[832a]
	Asp[100]	Glu[833]
	Ser[34]	None (a proline instead)
Phosphate	Tyr[50]	Tyr[783]
	Tyr[78]	Tyr[811]
	Arg[38]	Arg[771]
	Arg[41]	No electron density for Lys[774]
Indirect interactions	Glu[44] with Arg[38]	Glu[777] with Arg[771]

[a] These residues made a stacking interaction (3.9 Å) with the adenine ring.

explain the low affinity for ATP. Although hCASK-GK has a nearly complete conserved P-loop motif, several facts suggest that the P-loop is not competent to bind ATP. First, the strictly conserved lysine of the P-loop motif is absent. In hCASK, this residue is an arginine. Alignment of all known guanylate kinase sequences reveals strict conservation of the P-loop lysine. Second, the serine/threonine that follows the lysine in the P-loop motif is replaced by an arginine residue in hCASK. The role of a serine or threonine residue of the P-loop sequence is to participate in ATP binding by donating its hydroxyl side chain as a ligand to the magnesium ion that invariably accompanies ATP. The replacement of such a residue with an arginine in hCASK precludes the

ability of coordinating the magnesium ion. But perhaps more importantly, modeling of ATP in the hCASK-GK model (data not shown) reveals that the presence of the larger arginine side chain is not compatible with ATP binding. Third, hCASK-GK does not possess the arginine that would correspond to Arg-131 of yGMPK in the LID region. The function of this residue in yGMPK (and many other ATP-binding proteins) is to bind and position ATP by stacking against the adenine ring. Lastly, main-chain residues 891 and 892 from the CORE region of hCASK-GK, which correspond to residues 169 and 170 in yGMPK and participate in ATP binding, are not at the appropriate position to contribute to ATP binding. Although a conformational change of these residues to a

TABLE III
Binding partners of GK domain of different MAGUKs

Binding partner	MAGUK	References
Rabphilin3a	HCASK	(42)
Tbr-1	CASK (rat)	(29)
SPAR	PSD95	(43)
GKAPs, SAPAPs, and DAPs	PSD95, hDlg	(44–46)
GAKIN	HD1g	(28)
BEGAIN	PSD95/SAP90	(47)
MAP1A	PSD-93	(48)
Occludin	ZO-1 (human)	(49)
SH3 domain of Dlg	hCASK	(31)
SH3 domain of hCASK, PSD95, SAP97	hCASK, PSD95, SAP97 (intramolecular interaction)	(30, 31, 33)

more productive position for ATP interactions cannot be ruled out, this is unlikely because these residues are in the CORE region, which is rather rigid as exemplified by our comparison to yGMPK (see "Results"). Collectively, the above analysis presents a strong case against the ability of the P-loop like sequence of hCASK to act as a true P-loop and bind ATP. Thus, the low affinity binding of ATP to hCASK-GK can only be explained by ATP binding to the GMP-binding site.

Because hCASK-GK has an almost conserved GMP-binding site and it does bind GMP in equilibrium binding assays, we modeled GMP into the structure of hCASK-GK after a movement of the GMP-binding region based on the structure alignment between hCASK-GK and GMPK$_{GMP}$. After minor adjustment of side chains of some residues, most of the interactions observed between GMP and yGMPK in the GMPK$_{GMP}$ structure could be duplicated (Table II). The replacement of Ser-34 of yGMPK by a proline residue in hCASK-GK does not preclude GMP binding. Consistent with the absence of GMP bound to hCASK in our structure is the apparent disorder of residues 774–776, which are predicted to participate in GMP binding. Such binding usually leads to stabilization of relevant residues. Thus, our structure supports the results of *in vitro* binding studies. Extensive attempts at obtaining crystals that contain the complex between hCASK-GK and GMP failed. This observation is consistent with a GMP-induced conformational change in the GK domain that resulted in a species that unfortunately was not amenable for crystallization.

In conclusion, the structure of hCASK-GK reveals the similarities and differences between what has evolved to become a protein-binding module and its enzymatic predecessor. The lack of enzymatic activity, the weak ATP binding, and the high affinity to GMP is rationalized. The binding of GMP to hCASK-GK can be of high functional relevance by inducing conformational changes that serve to regulate MAGUKs, *i.e.* to influence the intermolecular interaction between GKAP and SAP-97 GK domain, between Tbr-1 and the CASK GK domain, or to influence the intramolecular interaction between the SH3 domain and the GK domain of SAP-97 and PSD95/SAP-90. If binding of GMP serves to regulate this inter- or intramolecular interaction, a possible mechanism would exist to regulate association of MAGUKs with various binding partners. This first structure of a MAGUK GK domain provides us with an example of a protein that has lost its enzymatic activity but maintained its ability to adjust its conformation upon ligand binding. The structural features shown by hCASK-GK may be common among other MAGUKs and are probably required for their function and regulation.

REFERENCES

1. Anderson, J. M. (1996) *Curr. Biol.* **6,** 382–384
2. De Lorenzo, C., Mechler, B. M., and Bryant, P. J. (1999) *Cancer Metastasis Rev.* **18,** 295–311
3. Dimitratos, S. D., Woods, D. F., Stathakis, D. G., and Bryant, P. J. (1999) *Bioessays* **21,** 912–921
4. Fujita, A., and Kurachi, Y. (2000) *Biochem. Biophys. Res. Commun.* **269,** 1–6
5. Gonzalez-Mariscal, L., Betanzos, A., and Avila-Flores, A. (2000) *Semin. Cell Dev. Biol.* **11,** 315–324
6. Stevenson, B. R., and Keon, B. H. (1998) *Annu. Rev. Cell Dev. Biol.* **14,** 89–109
7. Sheng, M., and Sala, C. (2001) *Annu. Rev. Neurosci.* **24,** 1–29
8. Guruprasad, L., Dhanaraj, V., Timm, D., Blundell, T. L., Gout, I., and Waterfield, M. D. (1995) *J. Mol. Biol.* **248,** 856–866
9. Kistner, U., Garner, C. C., and Linial, M. (1995) *FEBS Lett.* **359,** 159–163
10. Cohen, A. R., Woods, D. F., Marfatia, S. M., Walther, Z., Chishti, A. H., Anderson, J. M., and Wood, D. F. (1998) *J. Cell Biol.* **142,** 129–138
11. Brundiers, R., Lavie, A., Veit, T., Reinstein, J., Schlichting, I., Ostermann, N., Goody, R. S., and Konrad, M. (1999) *J. Biol. Chem.* **274,** 35289–35292
12. Doubie, S. (1997) **276,** 523–557
13. Matthews, B. W. (1968) *J. Mol. Biol.* **33,** 491–497
14. Otwinowski, Z., and Minor, W. (1997) *Methods Enzymol.* **276,** 307–326
15. Terwilliger, T. C., and Berendzen, J. (1999) *Acta Crystallogr. Sect. D Biol. Crystallogr.* **55,** 849–861
16. Cowtan, K. (1994) **31,** 34–38
17. Perrakis, A., Sixma, T. K., Wilson, K. S., and Lamzin, V. S. (1997) *Acta Crystallogr. Sect. D Biol. Crystallogr.* **53,** 448–455
18. Jones, T. A., Zou, J. Y., Cowan, S. W., and Kjeldgaard. (1991) *Acta Crystallogr. Sect. A* **47,** 110–119
19. Brunger, A., and Rice, L. (1997) *Methods Enzymol.* **277,** 243–269
20. Murshudov, G. N., Vagin, A. A., and Dodson, E. J. (1997) *Acta Crystallogr. Sect. D Biol. Crystallogr.* **53,** 240–255
21. Hendrickson, W., and Ogata, C. (1997) *Methods Enzymol.* **277,** 494–523
22. Blaszczyk, J., Li, Y., Yan, H., and Ji, X. (2001) *J. Mol. Biol.* **307,** 247–257
23. Kuhlendahl, S., Spangenberg, O., Konrad, M., Kim, E., and Garner, C. C. (1998) *Eur. J. Biochem.* **252,** 305–313
24. Husi, H., Ward, M. A., Choudhary, J. S., Blackstock, W. P., and Grant, S. G. (2000) *Nat. Neurosci.* **3,** 661–669
25. Husi, H., and Grant, S. G. (2001) *Trends Neurosci.* **24,** 259–266
26. Pawson, T., and Scott, J. D. (1997) *Science* **278,** 2075–2080
27. Garner, C. C., Nash, J., and Huganir, R. L. (2000) *Trends Cell Biol.* **10,** 274–280
28. Hanada, T., Lin, L., Tibaldi, E. V., Reinherz, E. L., and Chishti, A. H. (2000) *J. Biol. Chem.* **275,** 28774–28784
29. Hsueh, Y. P., Wang, T. F., Yang, F. C., and Sheng, M. (2000) *Nature* **404,** 298–302
30. McGee, A. W., and Bredt, D. S. (1999) *J. Biol. Chem.* **274,** 17431–17436
31. Nix, S. L., Chishti, A. H., Anderson, J. M., and Walther, Z. (2000) *J. Biol. Chem.* **275,** 41192–41200
32. Shin, H., Hsueh, Y. P., Yang, F. C., Kim, E., and Sheng, M. (2000) *J. Neurosci.* **20,** 3580–3587
33. Wu, H., Reissner, C., Kuhlendahl, S., Coblentz, B., Reuver, S., Kindler, S., Gundelfinger, E. D., and Garner, C. C. (2000) *EMBO J.* **19,** 5740–5751
34. Woods, D. F., and Bryant, P. J. (1991) *Cell* **66,** 451–464
35. Woods, D. F., Hough, C., Peel, D., Callaini, G., and Bryant, P. J. (1996) *J. Cell Biol.* **134,** 1469–1482
36. Thomas, U., Ebitsch, S., Gorczyca, M., Koh, Y. H., Hough, C. D., Woods, D., Gundelfinger, E. D., and Budnik, V. (2000) *Curr. Biol.* **10,** 1108–1117
37. Caruana, G., and Bernstein, A. (2001) *Mol. Cell. Biol.* **21,** 1475–1483
38. Lavie, A., Ostermann, N., Brundiers, R., Goody, R. S., Reinstein, J., Konrad, M., and Schlichting, I. (1998) *Proc. Natl. Acad. Sci. U. S. A.* **95,** 14045–14050
39. Corpet, F. (1988) *Nucleic Acids Res.* **16,** 10881–10890
40. Esnouf, R. M. (1997) *J. Mol. Graph. Model.* **15,** 132–134
41. Merritt, E. A., and Bacon, D. J. (1997) *Methods Enzymol.* **277,** 505–524
42. Zhang, Y., Luan, Z., Liu, A., and Hu, G. (2001) *FEBS Lett.* **497,** 99–102
43. Pak, D. T., Yang, S., Rudolph-Correia, S., Kim, E., and Sheng, M. (2001) *Neuron* **31,** 289–303
44. Takeuchi, M., Hata, Y., Hirao, K., Toyoda, A., Irie, M., and Takai, Y. (1997) *J. Biol. Chem.* **272,** 11943–11951
45. Satoh, K., Yanai, H., Senda, T., Kohu, K., Nakamura, T., Okumura, N., Matsumine, A., Kobayashi, S., Toyoshima, K., and Akiyama, T. (1997) *Genes Cells* **2,** 415–424
46. Kim, E., Naisbitt, S., Hsueh, Y. P., Rao, A., Rothschild, A., Craig, A. M., and Sheng, M. (1997) *J. Cell Biol.* **136,** 669–678
47. Deguchi, M., Hata, Y., Takeuchi, M., Ide, N., Hirao, K., Yao, I., Irie, M., Toyoda, A., and Takai, Y. (1998) *J. Biol. Chem.* **273,** 26269–26272
48. Brenman, J. E., Topinka, J. R., Cooper, E. C., McGee, A. W., Rosen, J., Milroy, T., Ralston, H. J., and Bredt, D. S. (1998) *J. Neurosci.* **18,** 8805–8813
49. Fanning, A. S., Jameson, B. J., Jesaitis, L. A., and Anderson, J. M. (1998) *J. Biol. Chem.* **273,** 29745–29753

MOLECULAR BASIS OF CELL AND
DEVELOPMENTAL BIOLOGY:

**Structural Basis for Nucleotide-dependent
Regulation of Membrane-associated
Guanylate Kinase-like Domains**

Yuanhe Li, Oliver Spangenberg, Ingo
Paarmann, Manfred Konrad and Arnon Lavie

Access the most updated version of this article at doi: 10.1074/jbc.M110792200

Find articles, minireviews, Reflections and Classics on similar topics on the JBC Affinity Sites.

Alerts:

- When this article is cited
- When a correction for this article is posted

Click here to choose from all of JBC's e-mail alerts

This article cites 47 references, 17 of which can be accessed free at
http://www.jbc.org/content/277/6/4159.full.html#ref-list-1